Project PAJ3 - Combined Cyclic Loading and Hostile Environments 1996-1999

Report No 11

Fractographic Analysis of Adhesive Joints

M R L Gower and W R Broughton

October 1999

NPL Report CMMT(A) 205

NPL Report CMMT(A)205
October 1999

Fractographic Analysis of Adhesive Joints

M R L Gower and W R Broughton
Centre for Materials Measurement & Technology
National Physical Laboratory
Teddington
Middlesex TW11 0LW, UK

ABSTRACT

This report details a programme of work carried out to characterise the combined effect of environmental exposure and mechanical loading on the microstructure of adhesives and adherend surfaces in joints. Joints were examined both before and after testing to failure or after interrupting tests to assess the level of damage accumulation. One acrylic and two epoxy based adhesives were used together with mild steel, carbon/epoxy composite, and aluminium and titanium alloy adherends to form a variety of joints. Three analysis techniques: (i) scanning electron microscopy (SEM); (ii) X-ray photoelectron spectroscopy (XPS); and (iii) X-ray refraction, were employed to examine whether physical/chemical changes in the appearance/structure of these surfaces, due to application of various loading and conditioning regimes, could be detected.

Results have shown that in general those joints based on mild steel (with the exception of T-peel joints) exhibited interfacial failure whilst aluminium and titanium alloy based joints tended to fail cohesively (with the exception of when F241 acrylic adhesive was used). For all joint configurations, the failure mode was independent of loading and conditioning regime used. SEM and XPS techniques were able to detect physical and chemical changes, respectively, in those adherends and adhesives effected by the various surface treatments and environmental conditioning regimes used. The X-ray refraction technique used for analysis of composite joints showed some promise, but further meaningful quantitative analysis will require specialist jigs and instrumentation.

The report was prepared as part of the research undertaken at NPL for the Department of Trade and Industry funded project on "Performance of Adhesive Joints - Combined Loading and Hostile Environments".

ISSN 1361 - 4061

National Physical Laboratory
Teddington, Middlesex, UK, TW11 0LW

Approved on behalf of Managing Director, NPL, by Dr C Lea,
Head of Centre for Materials Measurement and Technology.

CONTENTS

1. INTRODUCTION

This report details a programme of work carried out to characterise the microstructure of adhesives and adherend surfaces in joints, both before and after testing to failure to assess the level of damage accumulation. A variety of analysis techniques were used in the investigation:

- Scanning electron microscopy (SEM)
- X-ray photoelectron spectroscopy (XPS)
- X-ray refraction

Analysis was carried out on adhesively bonded joints that had been subjected to combinations of mechanical (static and cyclic) loading and environmental exposure (e.g. hot/wet). The purpose of the tests on the various joint configurations was to collect data on which statistical and analytical analyses could be performed and not to compare the relative merits or disadvantages of the various adhesives or adherends used.

The research discussed in this report forms part of the Engineering Industries Directorate of the United Kingdom Department of Trade and Industry project on "Performance of Adhesive Joints - Combined Cyclic Loading and Hostile Environments", which aims to develop and validate test methods and environmental conditioning procedures that can be used to measure parameters required for long-term performance predictions. This project is one of three technical projects forming the programme on "Performance of Adhesive Joints (PAJ) - A Programme in Support of Test Methods".

2. JOINT CONFIGURATIONS

A total of six adhesive joint configurations were analysed in this study: (i) single-lap; (ii) perforated single-lap; (iii) tapered-strap; (iv) thick adherend shear test (TAST); (v) T-peel; and (vi) scarf. Details of the joint configurations studied in the PAJ3 programme, the respective adhesive and adherend constituents and the loading and conditioning regimes used are given in Table 1. Only selected configurations were analysed and these are detailed in Section 7. Schematic diagrams and photographs of these joint types are depicted in Figures 1 to 12. It is noted here that although the thick adherend shear test can be performed in tension and compression, only tension specimens were examined. For all joint configurations, specimens were bonded in a jig. Holes were machined post cure and specimens were clamped in a vice during drilling. Sacrificial material was placed under the back face of specimens during drilling to prevent deformation.

3. ADHESIVES

The following adhesives were used in the PAJ3 programme.

(i) Araldite® 2007 (AV119): A one part epoxy adhesive supplied by Ciba Speciality Products. The cure schedule was 140^{o} C for 75 minutes.

(ii) F241: A toughened acrylic adhesive supplied by Permabond Adhesives Ltd. The adhesive was cured by applying an initiator to one surface and the acrylic resin to the other surface. The adhesive was allowed 24 hours to cure at room-temperature.

(iii) AF126-2: A modified epoxy film adhesive supplied by 3M, UK. The adhesive contains a carrier fabric for bondline thickness control. The cure cycle was 120^{o} C for 90 minutes.

It is noted that for the single-lap joints bonded with AV119, the bond-line thickness (0.25 mm) was controlled using 250 μm ballontini glass spheres. A small quantity of the glass spheres, 1% by weight, was mixed into the adhesive. Specimens were clamped in a special bonding jig and then heated to 140^{o} C for 75 minutes to cure the adhesive.

Table 1 Loading and Environmental Conditioning Regimes used in Test Programme

Joint configuration	Adherend/adhesive combinations	Loading	Conditioning
Single-lap	• mild steel + AV119 • mild steel + AF126-2 • titanium alloy + AF126-2 • T300/924 carbon/epoxy + AF126-2	Static tension	0, 3, 7, 14, 21 and 42 days @ 25, 40, 50, 60, 70° C distilled water immersion
		Tensile fatigue @ 25%, 40%, 55%, 70% and 80% ultimate strength	no conditioning
Perforated single-lap (3 x 3 mm ϕ holes)	• mild steel + AV119 • mild steel + AF126-2 • titanium alloy + AF126-2	Static tension	0, 3, 7, 14, 21 and 42 days @ 25, 40, 50, 60, 70° C distilled water immersion
		Tensile fatigue @ 25%, 40%, 55%, 70% and 80% ultimate strength	no conditioning
Tapered-strap	• aluminium 5251 + AF126-2	Static tensile	0, 42 days @ 70° C/85% relative humidity
		Tensile fatigue @ 55% ultimate strength	0, 42 days @ 70° C/85% relative humidity
Thick adherend shear (TAST)	• aluminium 5251 + AV119 • aluminium 5251 + AF126-2 • aluminium 5251 + F241	Static tension	0, 3, 7, 14, 21 and 42 days @ 25, 40, 50, 60, 70° C distilled water immersion
T-peel	• mild steel + AV119	Static tension	no conditioning
Scarf	• aluminium 5251 + AF126-2	Static tension	no conditioning
		Tensile fatigue @ 65%, 70%, 75%, 80%, and 85% ultimate strength	no conditioning

4. ADHERENDS

Adherends were machined from sheets of the following materials.

(i) Aluminium 5251 alloy supplied by Alcan.

(ii) CR1 cold rolled mild steel supplied by British Steel.

(iii) 6Al-4V-titanium alloy supplied by Titanium International Ltd.

(iv) T300/924 carbon/epoxy composite supplied by Hexcel Composites Ltd.

5. SURFACE TREATMENTS

The following surface treatments were used to prepare adherends for bonding:

Grit Blast and Degrease: Prior to bonding, the adherends were degreased with 1,1,1-trichloroethane and then grit blasted using 80/120 alumina to produce an uniform matt finish. A pressure of 85 psi was used to grit-blast the areas to be bonded. Any dust remaining after grit blasting was removed with clean compressed air. The surfaces to be bonded were then degreased again with 1,1,1-trichloroethane and dried. Specimens were bonded within one hour of grit blasting.

Grit Blast and A187 (g-glycidoxypropyltrimethoxy) Silane: The initial surface pre-treatment was identical to the procedure employed for grit blast and degrease. The grit blasted and degreased surface was subsequently coated with A187 silane coupling agent (supplied by Union Carbide). A 1% solution of A187 silane was prepared in deionised water and allowed to stand for 90 minutes to

hydrolyse. The solution was brushed onto the prepared surfaces. The coated adherends were then positioned to drain off the excess solution and allowed to dry in air for 2 to 3 hours before applying the adhesive.

Prior to bonding, the surfaces of the titanium and aluminium alloy sections to be bonded were chromic acid etched. A description of the technique is described below.

Chromic Acid Etch: Grit blasted and degreased specimens were immersed for 30 minutes in a chromic acid etch solution at a temperature of 60-70^{o}C. The specimens were removed from the etch solution and washed in cold tap water and then hot tap water. Finally, the specimens were rinsed with acetone and allowed to dry in a fan oven for a few minutes at 120^{o}C. Specimens were inverted to enable the water to drain from the areas to be bonded. The etch solution consisted of 500 ml of distilled water with 75 ml of sulphuric acid (H_2SO_4) and 37.5 g of sodium dichromate ($Na_2Cr_2O_7.2H_2O$).

It is noted here that fresh alumina grit was used each time an adherend was grit blasted.

6. ANALYSIS TECHNIQUES

The main objective of the work detailed in this report is to: (i) characterise the microstructure of the adhesive and adherend surfaces in the joint configurations studied and; (ii) to examine whether physical/chemical changes in the appearance/structure of these surfaces, due to application of the various loading and conditioning regimes, can be detected.

The analysis techniques used in this work are detailed below.

6.1. SCANNING ELECTRON MICROSCOPY (SEM)

Samples were initially viewed with the SEM to provide some basic information as to the morphology of treated metallic and adhesive fracture surfaces. Features of SEM are given below.

- SEM uses electrons rather than light to form an image.
- Used to obtain images of 3 dimensional surfaces due to the excellent depth of field capability of this technique.
- Resolution that can be obtained with SEM is approximately 100 times greater than for optical microscopy.
- Although SEM can be used to collect information about the types of atoms present in a sample, in this study the technique was only used in the capacity of providing images.

In all of the analyses carried out, the SEM (Camscan SII) was set up with a gun potential of 20 kV, a working distance of 21 mm and a beam resolution setting of 4. Specimen preparation is relatively straightforward. A conductive carbon adhesive is used to bond samples onto an aluminium stub which sits in a holder in the chamber of the microscope. If the sample being analysed is non-conductive, a conductive coating needs to be applied to the surface of the specimen to prevent charging by the electron beam. An anti-static spray was (in most cases) found to be satisfactory in preventing charge build up but a more effective gold-palladium coating was also used where this was not sufficient.

6.2. X-RAY PHOTOELECTRON SPECTROSCOPY (XPS)

- X-ray photoelectron spectroscopy (XPS) is an electron spectroscopic method that uses mono-energetic soft X-rays (magnesium radiation in this study) to eject electrons from inner-shell orbitals.
- Identification of the elements present in the sample can be made directly from the kinetic energy of ejected photoelectrons.

- Possible to identify the chemical state of elements from small variations in the kinetic energies of ejected photoelectrons.
- The relative concentration of the elements can be determined from the measured photoelectron intensities.
- For a solid, XPS probes 2 - 20 atomic layers deep, depending on: the material, the energy of the photoelectron concerned, and the angle (with-respect-to the surface) of the measurement (which in this case was 45^{o}).

XPS analysis was carried out in order to determine the chemical state of elements and the depth of the oxide layer present on the surfaces of aluminium and titanium samples that had undergone different surface treatments. In addition, aluminium TAST joints with three different adhesives having undergone environmental conditioning and testing were analysed. The XPS analyses were carried out at the University of Surrey, UK.

6.3. X-RAY REFRACTION

This technique is analogous to the refraction of light through transparent media such as prisms or lenses. X-rays are also refracted and penetrate materials far better than light. X-rays have very small scattering angles and a sensitivity for structures in the nanometer range. The intensity of the deflected X-rays is strongly dependent on the scattering angle which is dependent on the media through which the X-rays have passed. Therefore, X-ray refraction can be used to characterise heterogeneous materials such as composites (i.e. amount of fibre de-bonding, voids) by analysis of the refraction of X-rays at interfaces within the material. The technique cannot be used to analyse metallic samples as the X-rays are absorbed. Therefore, in this investigation composite lap joints have been analysed at the interface between adhesive and composite adherend to investigate whether conditioning under a hot/wet environment has a detrimental effect on the interface and/or the adhesive. For more detail on this technique and the experimental apparatus/set-up used the reader is referred to (1). This work has been kindly carried out by the Federal Institute for Materials Research and Testing, Berlin, Germany.

7. ANALYSES

Analyses were carried out on surface treated adherends and adhesive fracture surfaces on the various joints. Table 2 details which analyses were performed on the surface treated adherends and Table 3 details which techniques were used to analyse the various joint configurations.

Table 2 Surface treated adherends and analysis techniques used

Adherend	Surface treatment	Analysis technique(s)
titanium alloy	untreated	SEM
titanium alloy	grit blasted	SEM
titanium alloy	grit blasted + chromic acid etch	SEM, XPS
CR1 mild steel	none	SEM
CR1 mild steel	grit blasted	SEM
aluminium alloy	grit blasted	XPS
aluminium alloy	grit blasted + chromic acid etch	XPS
aluminium alloy	grit blasted + silane A187	XPS

Table 3 Joint configurations studied and analysis techniques used

Joint	Material combination(s)	Loading	Conditioning	Failure mode	Analysis techniques
Single-lap	CR1 mild steel + AV119	Static tension	none	interfacial	SEM
		40% UTS - tensile fatigue			
		55% UTS - tensile fatigue			
		80% UTS - tensile fatigue			
	T300/924 carbon/epoxy + AF126-2	Static tension	none	cohesive	X-ray refraction
		Static tension	1000 hours @ 70° C/85% RH		
Perforated Single-lap (3 x 3 mm ϕ holes)	CR1 mild steel + AV119	Static tension	7 days water immersion @ 25° C	interfacial	SEM
		Static tension	7 days water immersion @ 60° C		
		Static tension	42 days water immersion @ 25° C		
		Static tension	42 days water immersion @ 60° C		
Tapered-strap (double-overlap shear)	Al 5251 + AF126	Static tension	none	cohesive	SEM
		Static tension	42 days @ 70° C/85% RH		
		55% UTS - tensile fatigue followed by static tension	42 days @ 70° C/85% RH		
Thick adherend shear (TAST)	aluminium 5251 + AV119 (grit blasted)	Static tension	none	AV119 cohesive	SEM, XPS
	aluminium 5251 + AF126-2 (grit blasted)		42 days water immersion @ 25° C	AF126-2 cohesive	
	aluminium 5251 + F241 (grit blasted)		42 days water immersion @ 60° C	F241 interfacial	
	aluminium 5251 + AV119 (grit blasted + A187 silane)				
	aluminium 5251 + AF126-2 (grit blasted + A187 silane)				
	aluminium 5251 + F241 (grit blasted + A187 silane)				
T-peel	CR1 mild steel + AV119	Static tension	none	cohesive	SEM
Scarf	aluminium 5251 + AF126-2	Static tension	none	cohesive	SEM
		85% UTS - tensile fatigue	none		

N.B. - shaded box indicates that each TAST joint material combination was subjected to each of the three conditions listed.
UTS = ultimate tensile strength, RH = relative humidity.

8 RESULTS

8.1 ADHEREND SURFACE TREATMENTS

8.1.1 SEM Analyses

Initial examination of surface treated adherends was carried out using the SEM. Titanium and mild steel were studied to see if the effects of grit blasting and chromic acid etching could be observed. Grit blasting is performed to provide a much larger surface area for bonding and also removes weak oxide layers. A fine/matt surface finish was produced using the technique described in Section 5. This technique increases the mechanical adhesion compared to an untreated adherend. Chromic acid is a strong oxidising agent and the purpose of etching an adherend surface is to form an oxide layer on top of the base metal that will promote chemical bonding between the adherend and the adhesive.

Micrographs (Figures 13 to 15) show the surface topography of untreated titanium, titanium after grit blasting and titanium after grit blasting followed by chromic acid etch, respectively. Compared to the untreated surface, the grit blasted surface is much more pitted and granular. The chromic acid etched surface is not as rough as the grit blasted surface. The formation of an oxide layer (on top of the grit blasted surface) due to etching may explain the slightly smoother, more 'flaky' appearance. However, the SEM micrographs did not provide any information as to the depth of this oxide layer.

The only surface treatment applied to the mild steel was degrease and grit blast. Figures 16 and 17 are micrographs showing the surface appearance of untreated and grit blasted/degreased steel, respectively. The smooth, flat texture of the untreated steel is significantly transformed to a rough, pitted relief when grit blasted. This greatly increases the potential for mechanical adhesion. SEM micrographs depict the effect of grit blasting very clearly, but do not provide any information as to the chemical groups present on the adherend surfaces or the depth of oxide layer.

8.1.2 XPS Analyses

Aluminium and titanium adherends were analysed using XPS, having undergone the surface treatments listed in Table 2.

Surface surveys of the adherends studied produced plots of photoelectron binding energy (eV) against the number of counts. Identification of the elements present in the sample can be made directly from the binding energies. Closer analysis of significant peaks can identify the chemical state of the elements present from small variations in the binding energies. The relative concentration of the elements can also be determined from the measured photoelectron intensities.

Table 4 summarises the XPS results for the adherends analysed. The atomic percentages are calculated from the atomic ratios of the main peaks that were selected for closer analysis. In most cases additional smaller peaks were noted indicating the presence of other elements. These are noted in the comments column of Table 4. In all cases the elements present in the largest quantities are oxygen, carbon and the base adherend metal. The surveys showed that in all cases an oxide layer was present on the adherend and a carbon layer was also present on top of the oxide layer.

Typical XPS output plots for grit blasted aluminium are shown in Figures 18 to 22. Figure 18 shows the complete surface survey and the peaks recorded correspond to the groups present. Closer analysis of the main carbon peak (Figures 19 and 20) indicated that C-C, C-O, C=O and C-OH groups were present as contaminants. Figures 21 and 22 show the oxygen and aluminium peaks recorded. A small presence of sodium was discovered and this will most probably have been introduced onto the adherend surface by way of grease or sweat from handling of the sample. A small amount of nitrogen was also present and this may have been atmospheric or deposited during the grit blast process. The oxide layer was measured at 5.96 nm thick.

Table 4 XPS results for treated adherends.

Adherend (surface treatment)	ATOMIC %							COMMENTS
	C (1s)	O (1s)	Al (2p)	Si (2p)	Ti (2p)	N (1s)	Cl (2p)	
Al 5251 (grit blasted)	40.333	44.253	15.414	-	-	-	-	C-C, C -O, C=O and C -OH all present in carbon layer above oxide layer. Small amount of sodium (264) present, contaminant from ha ndling, grease, glass wear. Nitrogen present. **Oxide layer thickness is 5.96 nm.**
Al 5251 (grit blasted + chromic acid etch)	45.554	38.431	16.015	-	-	-	-	Carbon layer same as above. No sodium present. Nitrogen present. **Oxide layer thickness is 5.04 nm** . Small amount of sodium present.
Al 5251 (grit blasted + silane A187)	43.273	39.586	12.899	4.241	-	-	-	No C-OH group in carbon layer. Si present as expected. **Oxide layer thickness is 5.04 nm.**
Ti (grit blasted + chromic acid etch)	36.348	56.440	-	-	7.212	-	-	No check done for Si. Aluminium present - grit blast dust.

For the aluminium that had been grit blasted followed by chromic acid etch, the carbon layer contained the same groups as for the aluminium that had only been grit blasted. Again, small amounts of sodium and nitrogen were also present. The oxide layer was determined to be 5.04 nm thick.

The aluminium that had been silane treated did not contain the C-OH group in the carbon layer. As expected, Si was detected, present in the silane coupling agent. The oxide layer thickness was the same as for the acid etched aluminium at 5.04 nm.

Analysis of the titanium sample that had been grit blasted and chromic acid etched indicated that small traces of aluminium were present. This was most probably due to small amounts of alumina grit still present on the titanium sample.

Overall, the XPS analyses were successful in determining the oxide layer thicknesses for the aluminium samples (measurement of the oxide layer was not performed for the titanium sample). Surprisingly the oxide layer was thickest on the grit blasted aluminium sample as it was expected that chromic acid etch and silane treatments would have produced a thicker oxide layer as they are specialist oxidising techniques. This could be an artefact of not analysing the samples immediately after treatments. Useful data was generated as to the types and quantities of chemical elements/ groups present and indicated that a number of contaminants were present.

8.2 JOINT FRACTURE SURFACES

In general two types of adhesive bond fracture were observed in the joint configurations analysed. These were adhesive (interfacial) and cohesive failure modes. The respective failure modes for the joints studied are given in Table 3.
Adhesive failure occurs at the adhesive/adherend interface and is therefore alternatively termed an

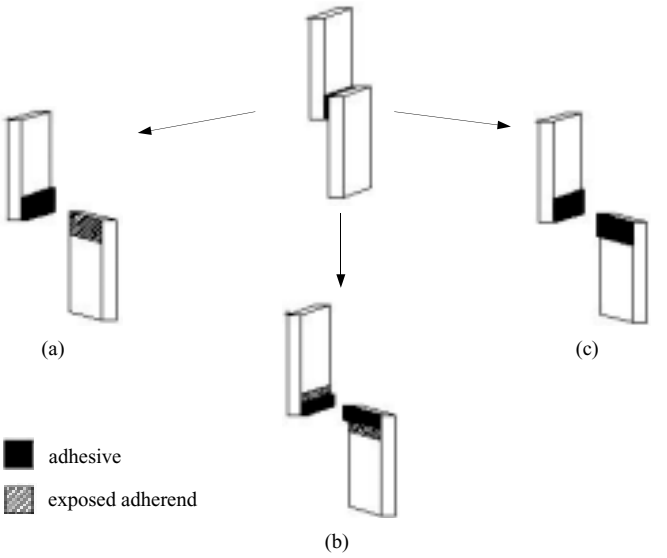

Figure 23 Typical generic fracture surfaces; (a), (b) interfacial failure, (c) cohesive failure

interfacial failure. This type of failure occurs as a result of a poor mechanical or chemical bond of the adhesive to the adherend. Generic interfacial fracture surfaces are illustrated in Figure 23 (a) and (b). In Figure 23 (a) the adhesive has failed along one adhesive/adherend interface leaving one adherend surface completely bare whilst the other is still covered with adhesive. Figure 23 (b) depicts the case where interfacial fracture occurs on both interfaces leaving regions on both adherends either covered with adhesive or bare. Figure 23 (b) is a simplified case where the adherend surfaces were 50% covered in adhesive and 50% bare metal. In practice it was observed that most interfacial failures left irregular patches of adhesive and exposed adherend on both adherend faces.

Cohesive fracture, where a crack is propagated through the adhesive layer leaving layers of adhesive bonded to both adherend surfaces is shown Figure 23 (c). A cohesive failure generally implies a good bond between adhesive and adherend.

Failure modes for all cases discussed in the following section are summarised in Table 3.

8.2.1 SEM Analyses

(i) Single-Lap Joints

CR1 mild steel/AV119 single-lap joints that had been tested under static tension and tensile fatigue were investigated using SEM. The aim of this analysis was to identify failure modes for the different loading regimes. Several specimens were examined and the appearance of the fracture surfaces showed considerable variation. However, all failures were interfacial and a general fracture pattern was noted. Figures 24 to 27 (micrographs of fracture surfaces in the centre of the overlap region - corresponding to shaded region of Figure 8) are typical of those observed. Figure 24 shows the fracture surface for a specimen that had been monotonically loaded to failure in tension. The fracture surface is fairly flat across the width of the joint. Looking at the fatigued samples (Figures 25 to 27), it is apparent that the fracture surfaces are slightly more raised than for the static case. In addition, instead of the fracture surfaces being sharp peaks and plateaus, they are generally smooth and 'roll' shaped. This is considered to be due to the action of the cyclic tensile load. Fracture was observed as initiating from the fillet regions at the edges of the overlap region (see Figures 25 and 26) and in most cases fracture occurred in a clear cut interfacial manner on one side of the overlap region (marked as region A on Figures 25 and 26), changing to a more patchy interfacial pattern on the other side (region B). The relative positions of regions A and B are shown in Figure 8. For the fatigue samples there is evidence of plastic yielding in the adhesive. The ballontini glass spheres used to control bond-line thickness are apparent in the micrographs giving a slight pock marked appearance in regions of adhesive.

(ii) Perforated Single Lap Joints

SEM micrographs of the perforated single lap joints studied are shown in Figures 28 to 31. It is clear from these micrographs that all failures were interfacial in nature. The effects of variation in water immersion period and temperature, if any, could not be ascertained from the SEM analyses performed. There are indications of localised yielding, although small, around the drilled holes. The peel stresses in these regions are slightly raised in comparison with the surrounding material. However, the stresses are far lower than those present at the ends of the overlap. There was no gross yielding of the adherend between holes. In some cases, striations were present on the adhesive surface in the region between the holes. In Figure 28 the voids clearly seen within the drilled holes are an artefact of the preparation procedure for producing SEM specimens.

(iii) Tapered-Strap

Three aluminium joints were analysed. The conditioning and loading regimes for these specimens

are detailed in Table 3. The SEM micrographs for these specimens are shown in Figures 32 to 34. For the specimens conditioned at 70°C/85% relative humidity the appearance of the fracture surfaces were similar despite the difference in loading regime. The carrier fabric for these specimens, has in many places, de-bonded from the adhesive to give a 'fluffy' surface appearance. This was not the case for the unconditioned specimen tested in static tension.

(iv) Thick Adherend Shear Test (TAST)

Details of the different test configurations considered are detailed in Table 3. Micrographs of each specimen analysed were produced. Differences between the appearance of the two different surface treatments (grit blast and grit blast + A187 silane) for the three adhesive systems assessed could not be distinguished. Therefore only the micrographs of the grit blasted specimens have been included in this report. These micrographs are shown in Figures 35 to 43.

Figures 35 to 37 show typical fracture surfaces for the aluminium 5251 alloy + AV119 specimens after different levels of environmental conditioning. As previously stated, aluminium TAST specimens with AV119 adhesive showed a predominantly cohesive failure with a slight amount of interfacial fracture. The mode of failure was independent of conditioning regime. Figure 35 shows the fracture surface of a TAST specimen having undergone no conditioning and both cohesive and interfacial fracture can be seen. Figure 36 depicts an area of interfacial fracture on the failure surface of a specimen tested after 42 days exposure to water at 25°C whilst Figure 37 illustrates the largely cohesive type of failure typical of aluminium 5251 alloy + AV119 TAST specimens.

Figures 38 to 40 show the failure surfaces of aluminium 5251 alloy + AF126-2 TAST specimens. The failure mode is cohesive and independent of conditioning regime as the figures show.

Figures 41 to 43 are micrographs of Al 5251 + F241 specimens. All failures were interfacial with failure always occurring at the interface corresponding to the surface on which the adhesive had been applied - see Section 3. It is apparent from the micrographs that changes in the structure of the adhesive occur when specimens immersed in water at elevated temperatures. A transition can be seen from the unconditioned state (Figure 41) through to 42 days in water at 60°C (Figure 43). As the length of exposure increases, the surface of the adhesive becomes 'flaky' and then rather granular. The manufacturers of F241 adhesive could not wholly explain (2, 3) this phenomena, but it is thought that exposure to temperatures above 60°C can cause some degradation of the adhesive. The F241 adhesive is based on a chlorosulphonated rubber with a methyl methacrylate resin and water immersion may cause some hydrolysis of the methyl methacrylate resin resulting in swelling of the resin. The combination of elevated temperature and immersion to water is likely to be the cause in the change of structure of the adhesive. It was observed that the strength of the joint initially increased before steadily decreasing with exposure time. This is an indication that the adhesive was post curing during the early stages of conditioning.

According to the manufacturer, F241 adhesive should be a white colour if the correct proportions of adhesive and initiator have been used. If too much initiator is used then the adhesive is usually a light brown or caramel colour. The adhesive resin absorbs the initiator on application and any excess initiator will spread out over the surface of the adhesive like an oil film. If this occurs then a weak layer will be formed between the adhesive and the adherend, reducing the strength of the bond. However, as all the bonds failed on the adhesive side, it is most likely that the correct amount of initiator was used and the brown colouring was as a result of the adhesive being exposed to light after failure.

(v) T-Peel Joint

The CR1 mild steel/AV119 joint analysed failed cohesively. This was somewhat surprising as poor adhesion had been observed for single-lap joints with similar surface preparation and as the

adherence of the oxide layer to the metal substrate was poor. The photograph in Figure 44 shows that cohesive failure initiates in the adhesive fillet where the two L shaped adherends first converge rather than at the interface. For most specimens crack propagation was cohesive except for 42 days exposure at 70^{o}C/85% relative humidity. SEM micrographs of the failure surfaces of the T-peel joint were very similar in appearance to Figure 37.

(vi) Scarf Joint

Two aluminium 5251 alloy + AF126-2 scarf joints were analysed. One of the joints was tested in static tension and the other at tensile fatigue (85% ultimate tensile strength). Both joints failed cohesively and micrographs of the fracture surfaces are shown in Figures 45 and 46. It was not possible to identify any distinguishing surface features to differentiate the two test conditions (both surfaces presented areas identical to those shown in Figures 45 and 46). The crack initiation region was not noticeably different from areas within the bulk of the adhesive joint.

8.2.2 XPS Analyses

Aluminium TAST specimens were analysed using XPS to investigate whether chemical changes could be detected in the three adhesives after 42 days water immersion at 60^{o}C - the harshest conditioning regime used. The same technique was used as for the XPS analyses carried out on the surface treated adherends. The results are shown in Table 5.

The first observation to make is that no aluminium was detected in the surveys. This was because the adhesive on top of the adherend was thick enough to prevent emission of electrons from the adherend. Only elements that are present in the adhesive layer are detected.

For the F241 TAST specimens, the proportions of carbon and oxygen did change on conditioning, with there being an increase of approximately 5% in the amount of oxygen detected and a similar decrease in the proportion of carbon present. As previously stated in section 8.2.1, the change in appearance of the F241 adhesive when immersed in water at elevated temperatures, was hypothesised as being a result of hydrolysis of the methyl methacrylate component of the resin. This theory is given more credence when the XPS results are considered. Hydrolysis can be expected to cause this increase in the oxygen level.

Although the glass transition temperature for both AV119 and AF126-2 adhesives decreases with increasing moisture content, there was no evidence of any chemical changes using XPS. The XPS results reflect the observations made with SEM.

8.3 X-RAY REFRACTION

Carbon/epoxy composite single lap joints, with AF126-2 adhesive, were analysed using the X-ray refraction technique. It should be noted here that the work carried out with X-ray refraction was exploratory work to investigate if the technique could be used to detect any changes in the adhesive/ adherend interface. Conditioned and unconditioned specimens were tested in static tension at NPL and the results recorded. Failure in both cases was cohesive and a reduction in strength was noted for the conditioned specimens as expected. X-ray refraction analyses were carried out on conditioned and unconditioned specimens which had not been tested to determine the degree of degradation. Specimens were inspected in two modes: (i) transverse topographs were taken (Figure 47 (a)) across the width of the specimens; and (ii) grazing incidence topographs were taken parallel to the joint plane (Figure 47 (b)). Transverse topographs of the carbon/epoxy adherend show no evidence of damage (i.e. transverse cracking) within the composite adherends in the bond area.

Scattering perpendicular to the fibre longitudinal axis (not shown in Figure 47) revealed no fibre de-bonding after conditioning in any region of the specimen. Earlier studies with CFRP laminates (4) have reported fibre de-bonding occurring after much longer conditioning times; typically ~10,000 hours.

Table 5 XPS results for aluminium TAST specimens

Thick adherend shear test (TAST) specimen	Atomic %							Comments
	C (1s)	O (1s)	Al (2p)	Si (2p)	Ti (2p)	N (1s)	Cl (2p)	
aluminium 5251 + AV119 - no conditioning	70.476	20.132	-	7.184	-	2.208	-	No metal seen, just large C peak due to adhesive.
aluminium 5251 + AV119 - 42 days water immersion @ 60° C	70.526	19.099	-	5.994	-	4.380	-	
aluminium 5251 + AF126 - no conditioning	76.608	17.089	-	2.964	-	3.339	-	
aluminium 5251 + AF126 - 42 days water immersion @ 60° C	78.369	17.123	-	1.367	-	3.140	-	
aluminium 5251 - F241 - no conditioning	79.980	13.555	-	3.710	-	0.736	2.019	Chlorine and sulphur present - from chlorosulphonated rubber. Nitrogen from pyridine initiator.
aluminium 5251 - F241 - 42 days water immersion @ 60° C	75.683	18.745	-	1.253	-	1.121	3.199	Chlorine present - from chlorosulphonated rubber. Small amount of flourine present. Nitrogen from initiator.

Grazing incidence topographs reveal strong signals from the joint interface. However, the signal depends strongly on the precise orientation of the specimen parallel to the beam and therefore any differences that would hoped to be detected after conditioning can not be measured with sufficient reliability. A special jig and instrumentation for precise inclination of the specimen in relation to the beam would be needed for a quantitative interpretation.

9. CONCLUSIONS

Three analysis techniques have been used in order to characterise the microstructure of various joint configurations fabricated from metallic and composite adherends with epoxy and acrylic based adhesives. Various conditioning and loading regimes were used. SEM and XPS are capable of showing changes in the physical and chemical structures, respectively.

Results have shown that in general those joints based on mild steel (with the exception of the T-peel joints) exhibited interfacial failure. This is due to weak adhesion to the base metal of the thick oxide layer that forms on steel and suggests that better surface preparation is needed to remove this layer. All joints that were based on aluminium and titanium adherends and that used epoxy based adhesives failed cohesively. This is due to fact that the thinner oxide layers that develop on aluminium and titanium form a much stronger bond to the base metal than is the case with steel. SEM analyses showed the benefit of grit blasting for increased mechanical adhesion, whilst XPS analyses showed that for the samples analysed in this study, the thickness of the oxide layer could be easily determined.

For all joint configurations, the failure mode was independent of loading and conditioning regime used. Epoxy based adhesives, although exhibiting a change in transition temperature after water immersion, showed no differences in structure or chemical composition after conditioning. However changes were detected for the acrylic based adhesive.

Results achieved in the exploratory work indicate that the X-ray refraction technique shows promise. However, it is clear that if meaningful quantitative data is to be collected then further studies would require specialist jigs and instrumentation for accurate alignment of specimens.

ACKNOWLEDGEMENTS

This work forms part of a programme on adhesives measurement technology funded by the Department of Trade and Industry as part of its support of the technological competitiveness of UK industry. The authors would like to express their gratitude to all members of the Industrial Advisory Group (IAG) and to the members of UK industry outside the IAG, whose contributions and advice have made this report possible. The authors gratefully acknowledge the help of Dr John Watts and Mr Steven Greaves of Surrey University, UK and the work carried out by Dr Manfred Hentschel and Dr Wolfram Harbich of the Federal Institute for Materials Research and Testing, Berlin, Germany. Other DTI funded programmes on materials are also conducted by the Centre for Materials Measurement and Technology, NPL as prime contractor. For further details please contact Mrs G Tellet, NPL.

REFERENCES

1. M. P. Hentschel, K.-W. Harbich and A. Lange, “Non-destructive evaluation of single fibre de-bonding in composites by X-ray refraction”, NDT&E International, 1994 Volume 27, Number 5, pp275-280.

2. Private communications with Professor Bill Lees, October 1999.

3. Private communications with Dr Terry Baldwin, Permabond, October 1999.

4. Private communications with Dr Manfred Hentschel, Federal Institute for Materials Research and Testing, Berlin, Germany, August - October 1999.

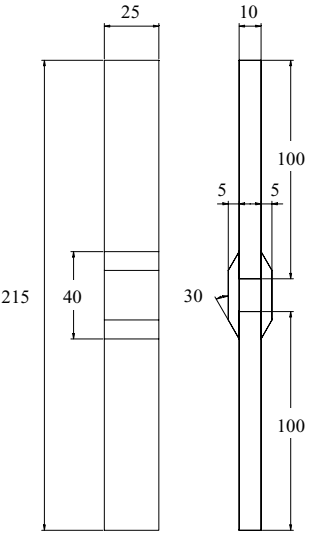

Figure 1 Schematic of tapered-lap joint

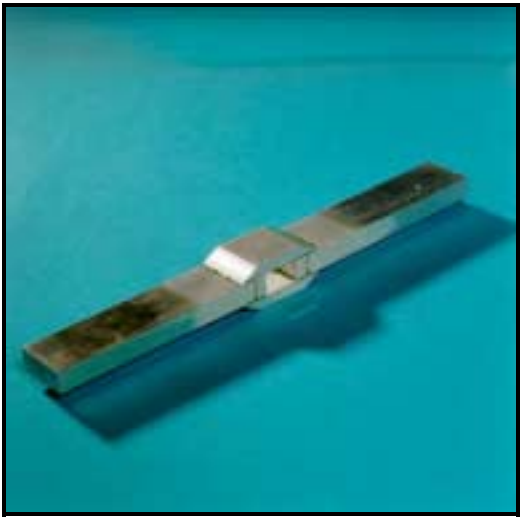

Figure 2 A typical tapered-lap joint.

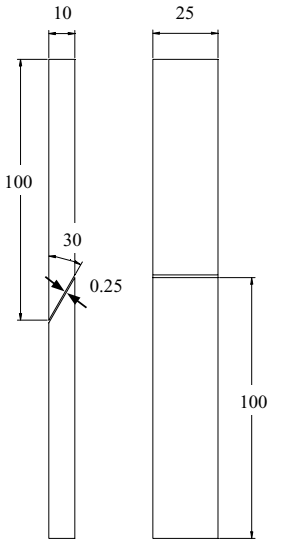

dimensions in millimetres

Figure 3 Schematic of scarf joint with taper angle of 30°.

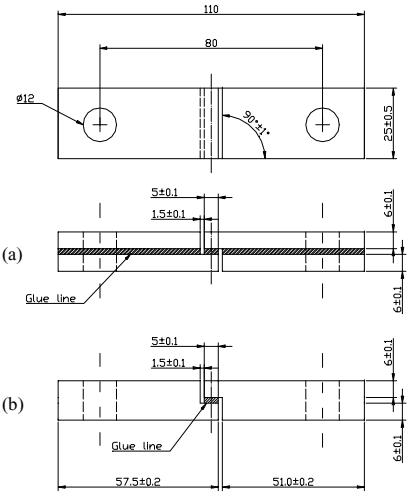

dimensions in millimetres

Figure 4 TAST specimen (tension): (a) bonded adherends; (b) pre-shaped adherends.

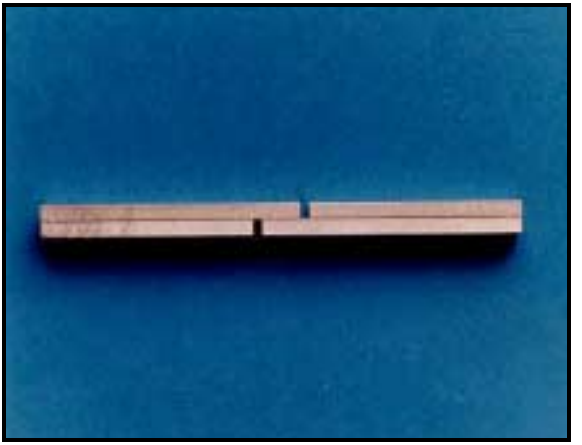

Figure 5 A typical tension TAST specimen (side view).

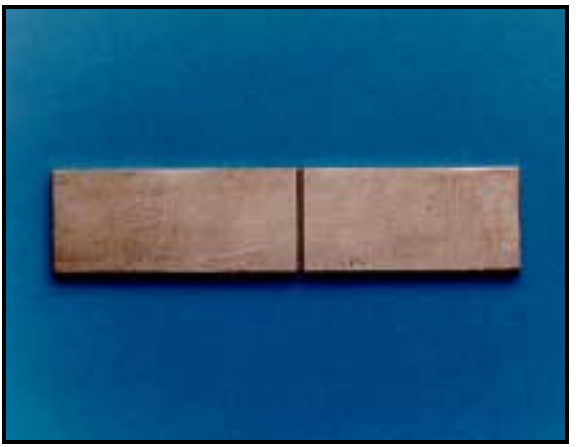

Figure 6 A typical tension TAST specimen (plan view).

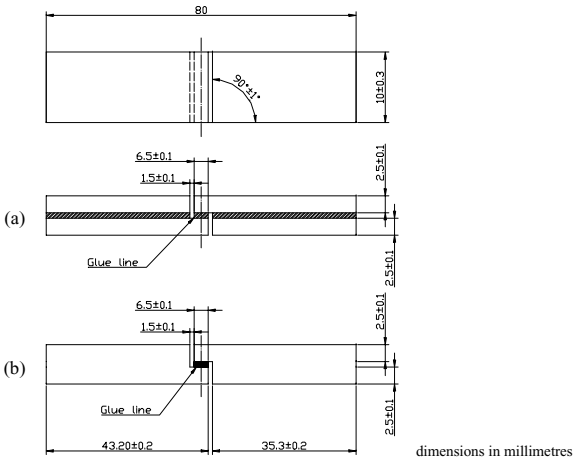

Figure 7 TAST specimen (compression): (a) bonded adherends; (b) pre-shaped adherends.

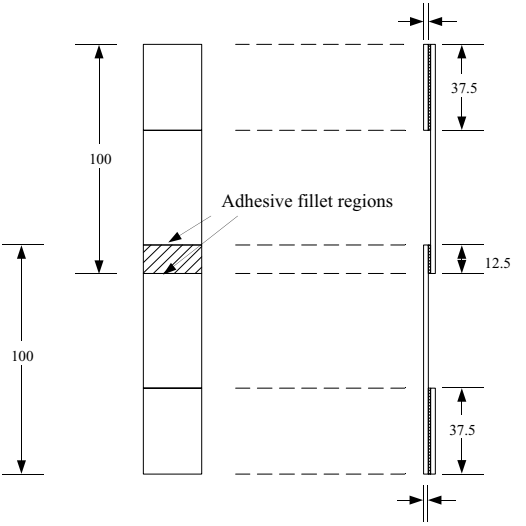

Figure 8 Schematic of single lap joint

Figure 9 A typical single lap joint

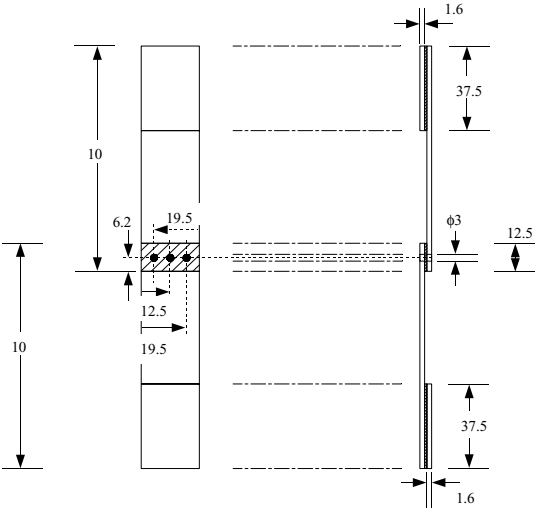

Figure 10 Schematic of perforated single lap joint

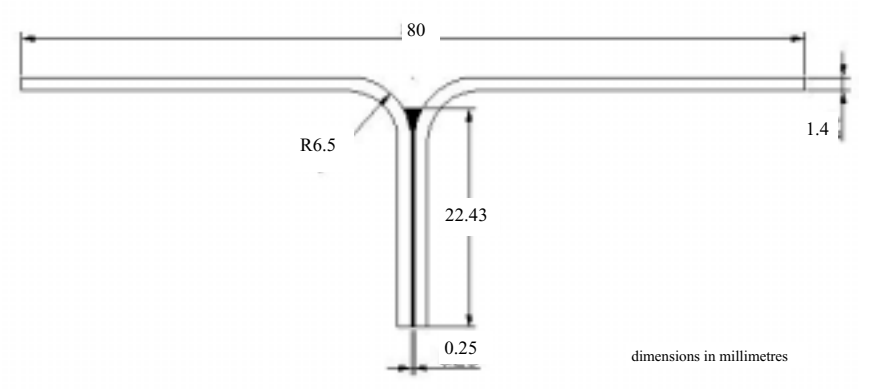

Figure 11 Schematic of T-peel joint

Figure 12 A typical T-peel joint.

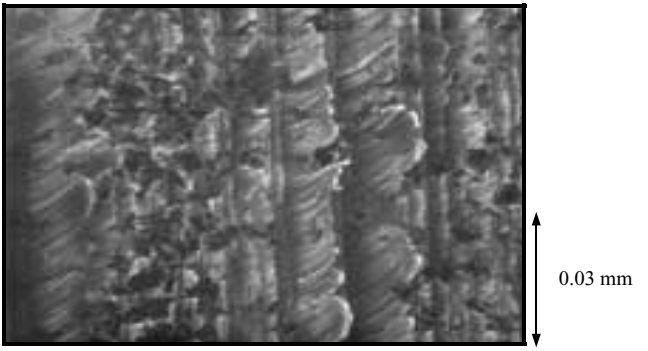

Figure 13 Surface appearance of untreated titanium (x 900 magnification)

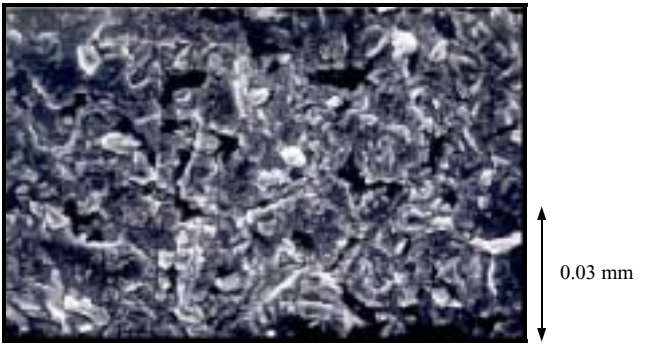

Figure 14 Surface appearance of grit blasted titanium (x 900 magnification)

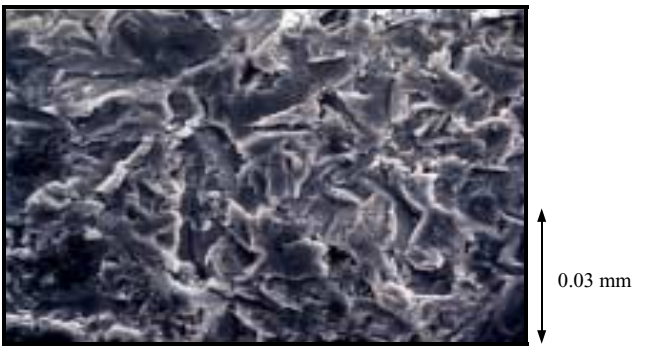

Figure 15 Surface appearance of titanium after grit blasting followed by chromic acid etch. (x 900 magnification)

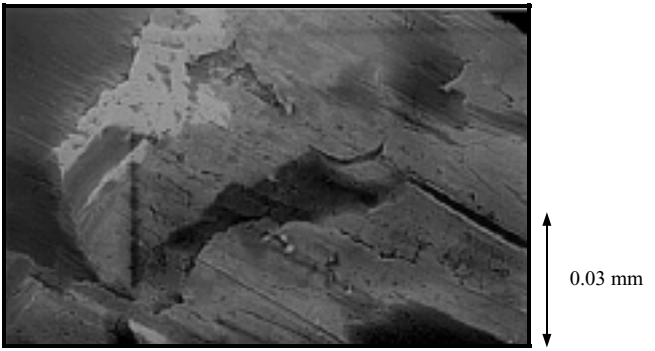

Figure 16 Surface appearance of mild steel - untreated. (x 900 magnification)

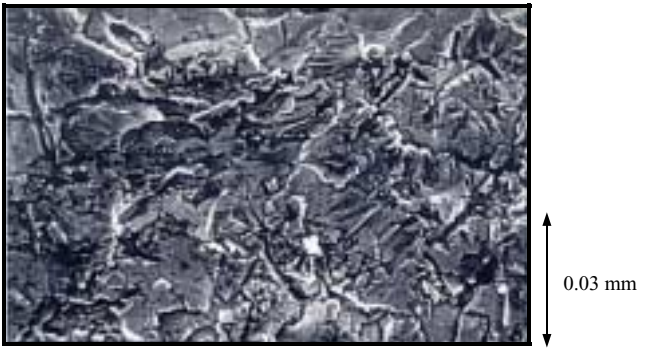

Figure 17 Surface appearance of grit blasted mild steel (x 900 magnification)

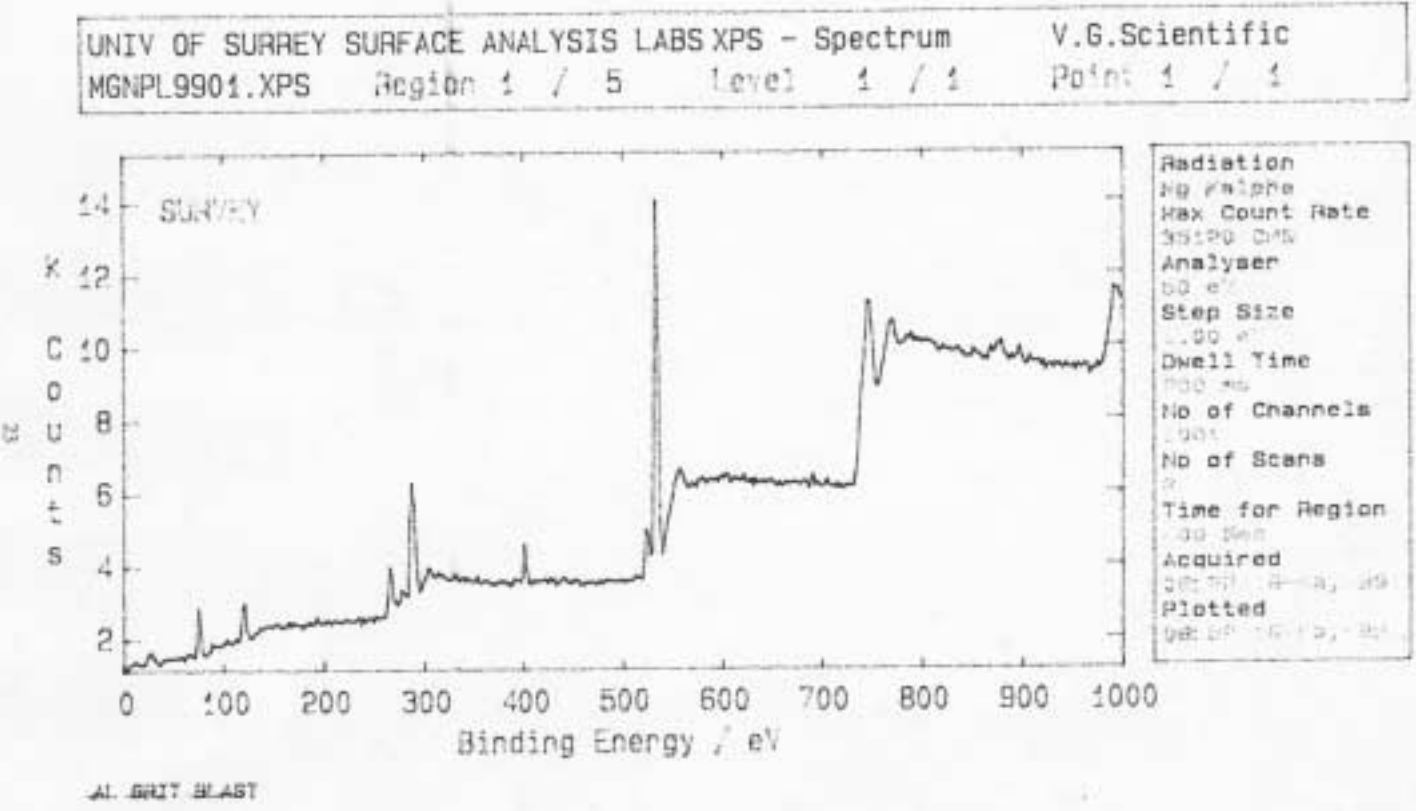

Figure 18 XPS surface survey for grit blasted aluminium 5251 alloy.

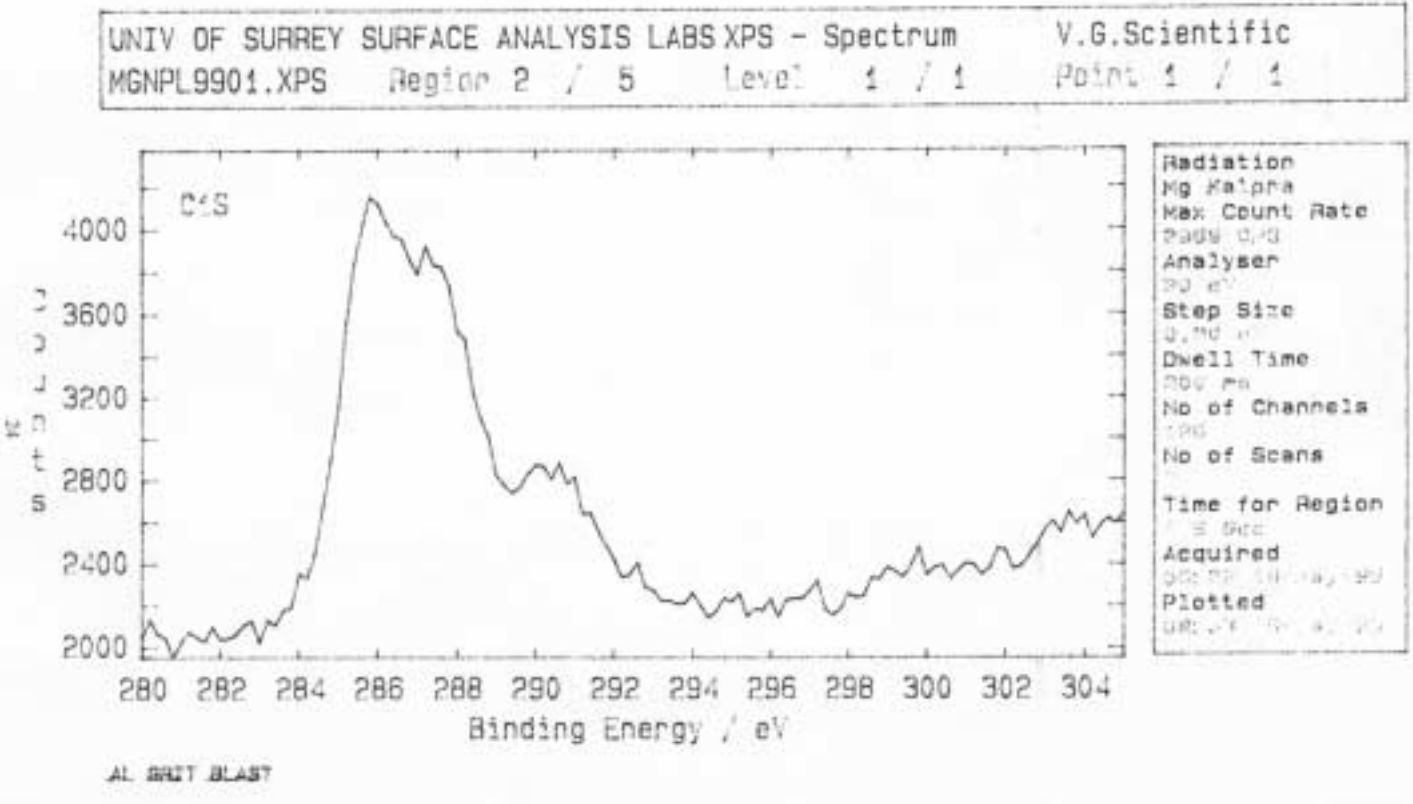

Figure 19 XPS carbon peak for grit blasted aluminium 5251 alloy.

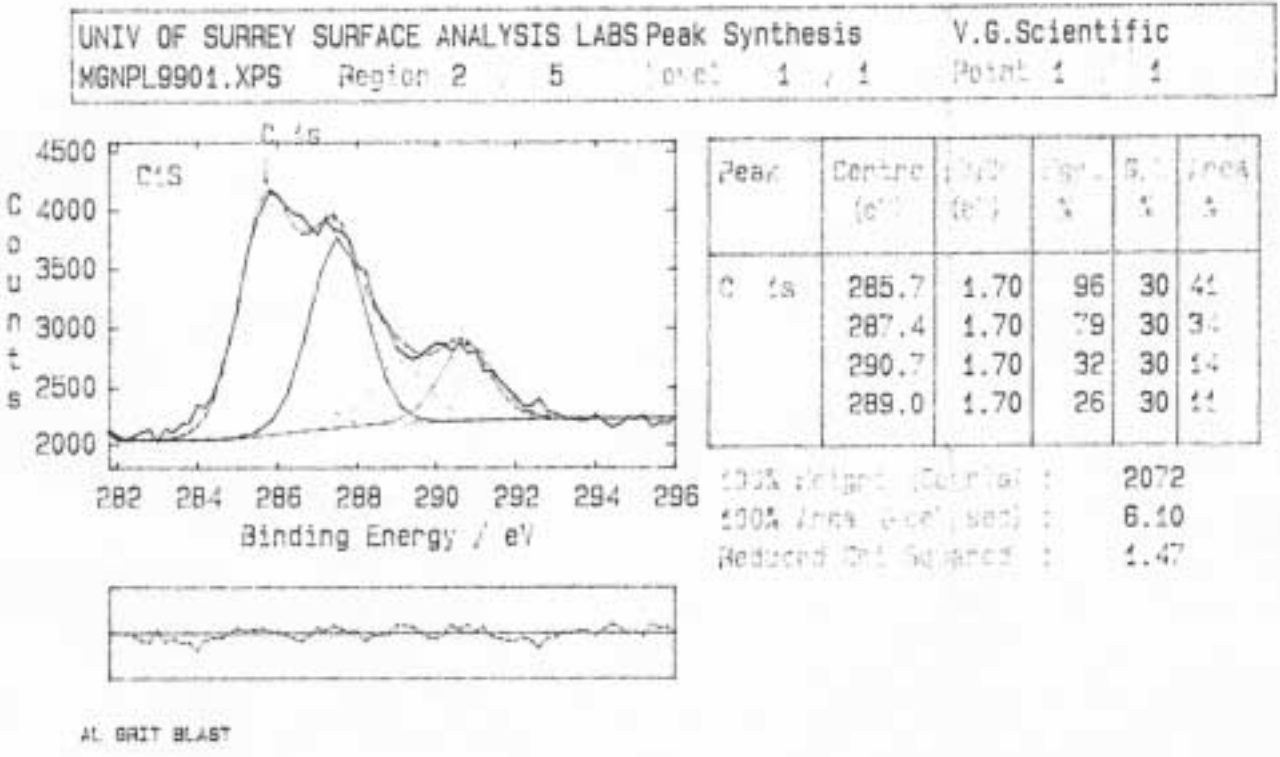

Figure 20 XPS main carbon peak for grit blasted aluminium 5251 alloy showing separate peaks corresponding to C-C, C-O, C=O and C-OH groups.

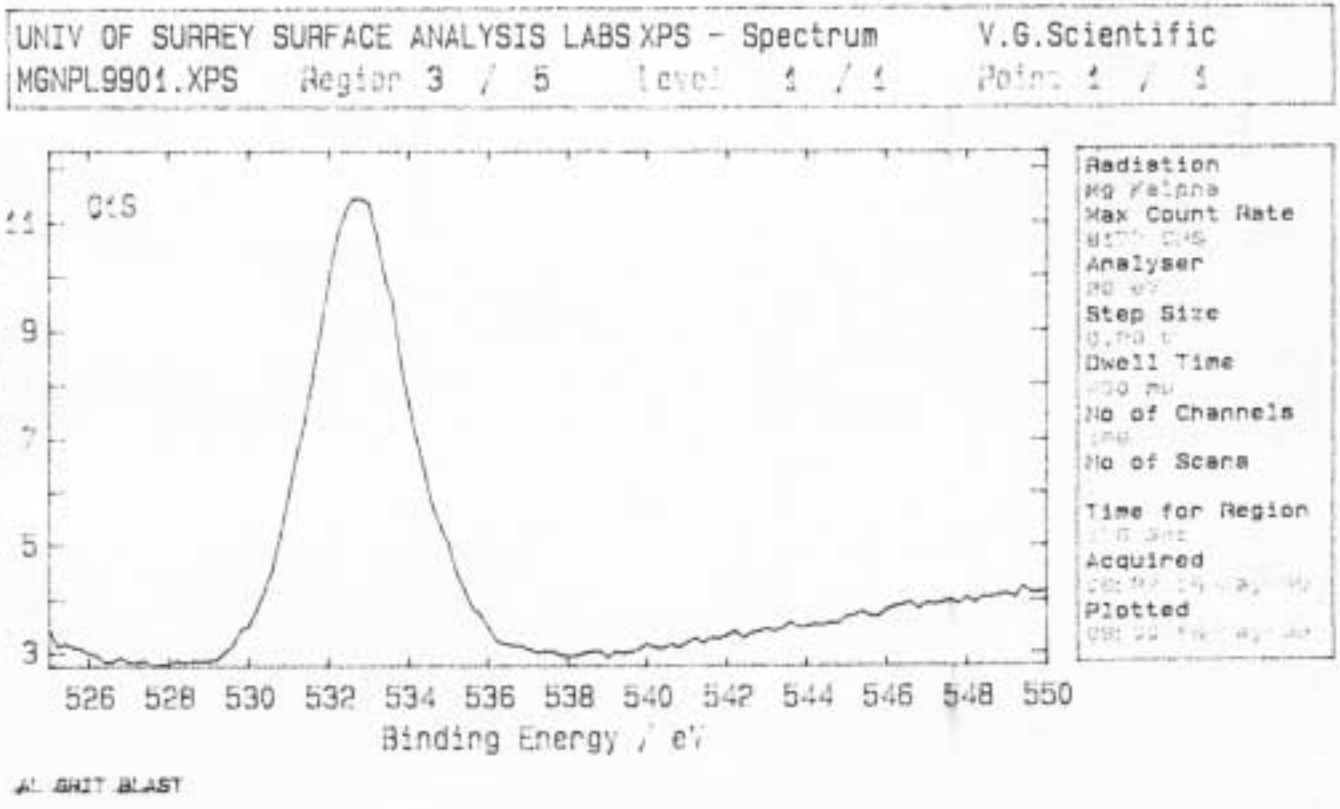

Figure 21 XPS oxygen peak for grit blasted aluminium 5251 alloy.

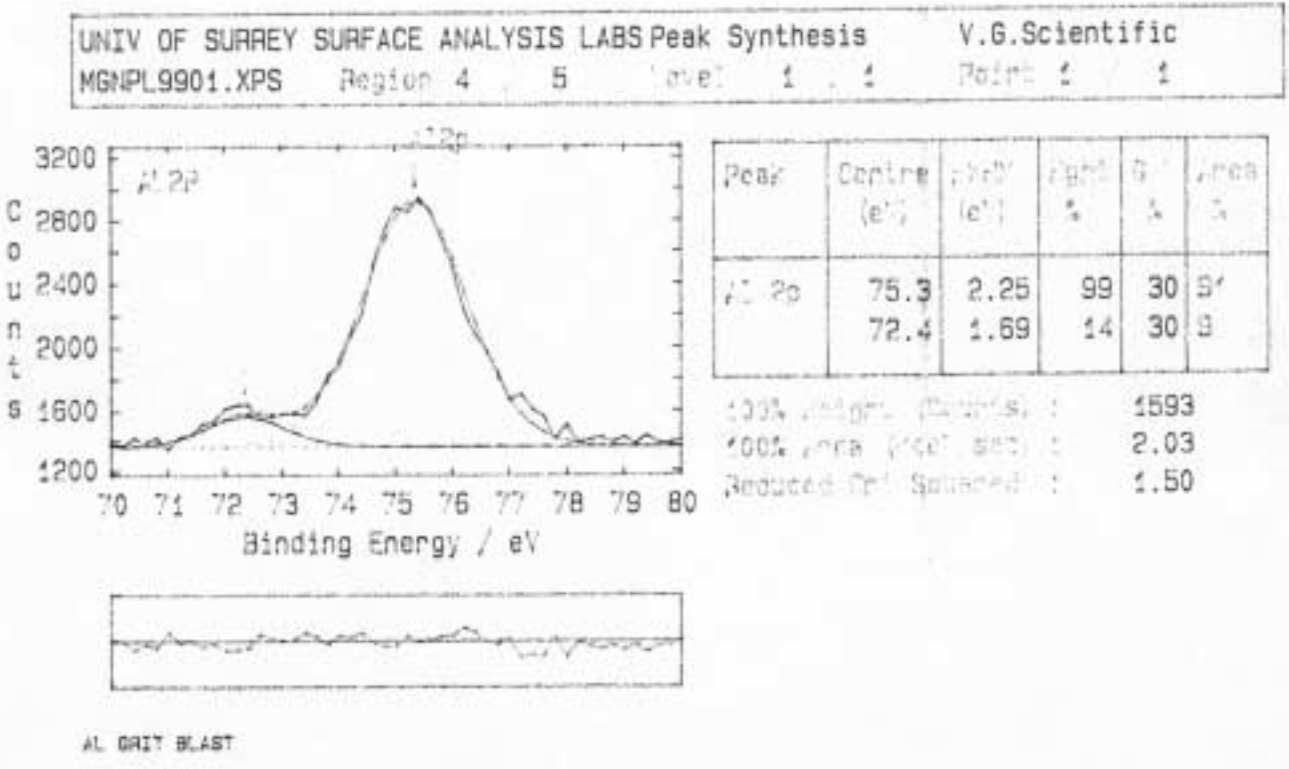

Figure 22 XPS aluminium peak for grit blasted aluminium 5251 alloy.

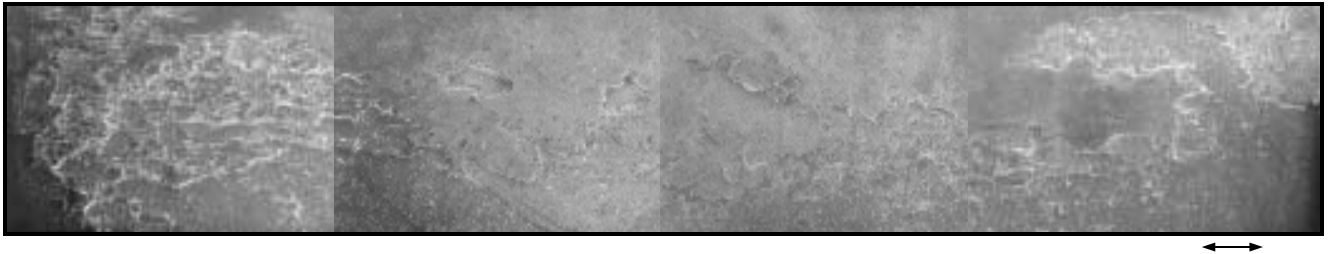

Figure 24 A typical micrograph of the interfacial fracture of a CR1 mild steel/AV119 single lap joint tested in static tension. 1 mm

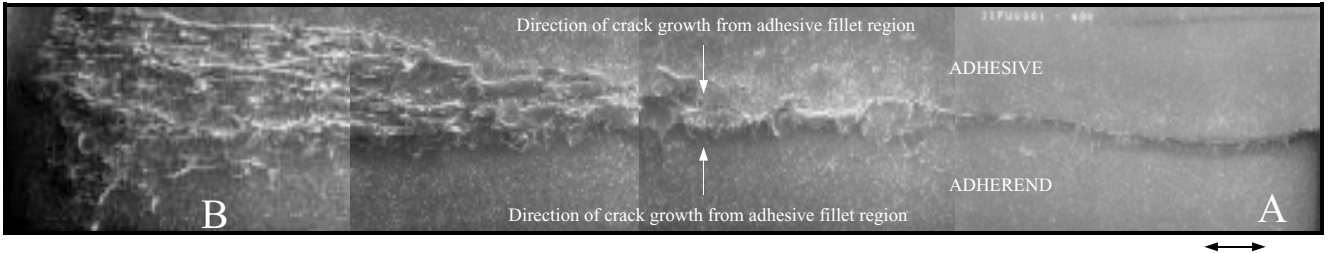

Figure 25 A typical micrograph of the interfacial fracture of a CR1 mild steel/AV119 single lap joint tested at 40% tensile fatigue. 1 mm

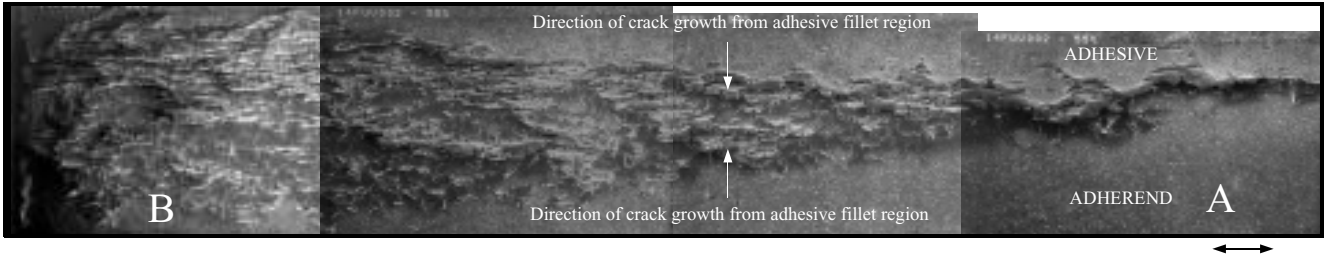

Figure 26 A typical micrograph of the interfacial fracture of a CR1 mild steel/AV119 single lap joint tested at 55% tensile fatigue.

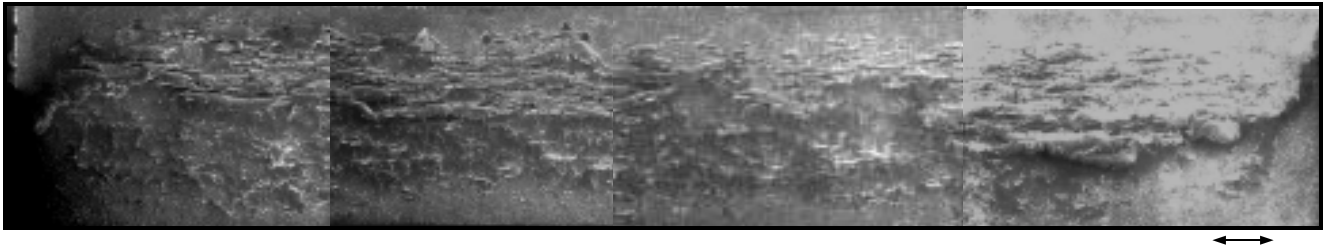

Figure 27 A typical micrograph of the interfacial fracture of a CR1 mild steel/AV119 single lap joint tested at 80% tensile fatigue.

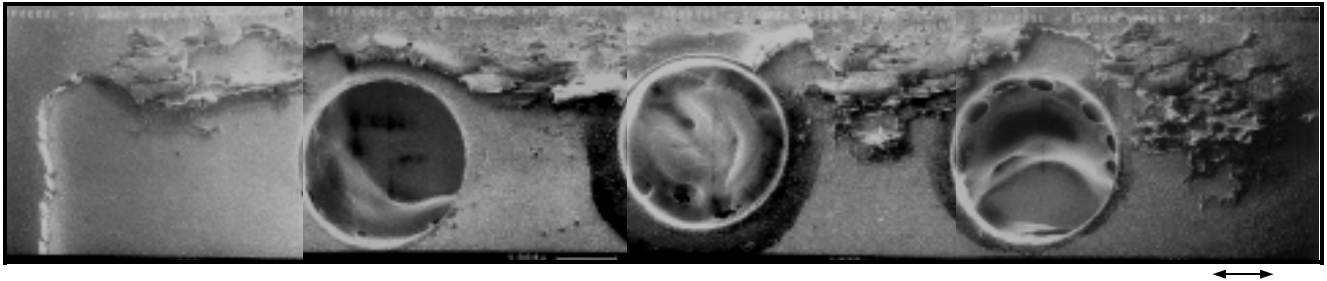

Figure 28 A typical micrograph of the interfacial fracture of a CR1 mild steel/AV119 perforated lap joint tested in static tensi on after 7 days of water immersion at 25° C.

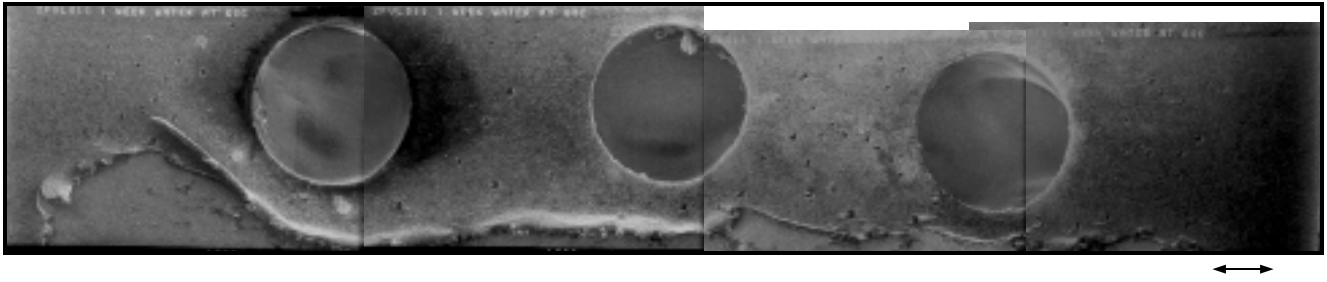

Figure 29 A typical micrograph of the interfacial fracture of a CR1 mild steel/AV119 perforated lap joint tested in static tensi on after 7 days of water immersion at 60° C.

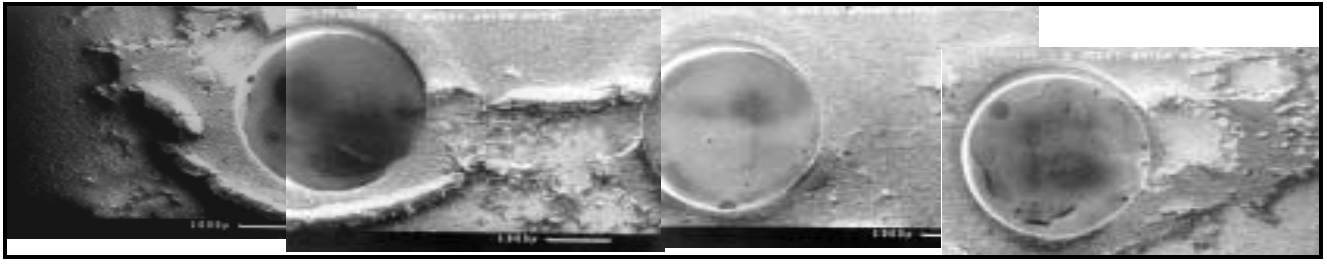

Figure 30 A typical micrograph of the interfacial fracture of a CR1 mild steel/AV119 perforated lap joint tested in static tensi on after 42 days of water immersion at 25° C.

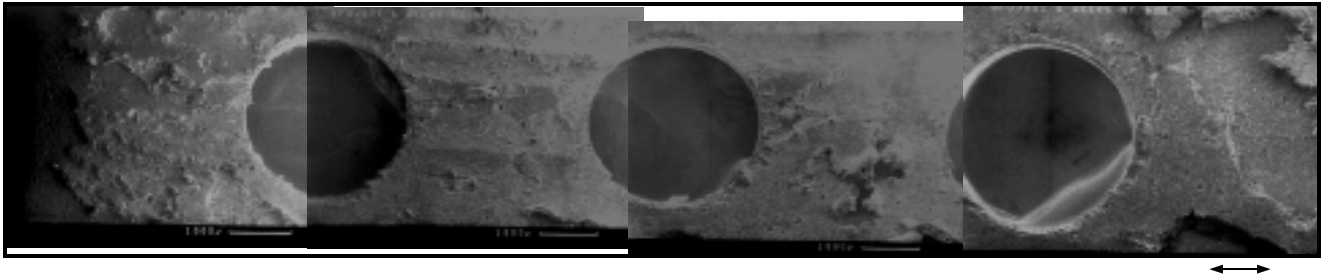

Figure 31 A typical micrograph of the interfacial fracture of a CR1 mild steel/AV119 perforated lap joint tested in static tensi on after 42 days of water immersion at 60° C.

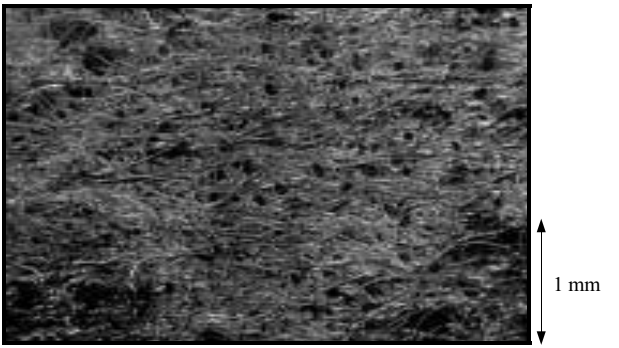

Figure 32 Typical fracture surface of an Al 5251/AF126 unconditioned tapered-strap joint specimen, tested in static tension. (x24 magnification).

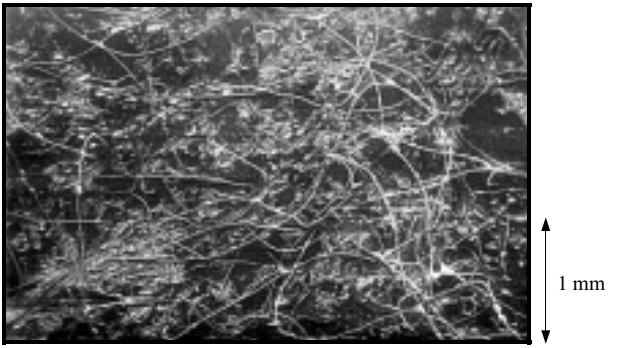

Figure 33 Typical fracture surface of an Al 5251/AF126 tapered-strap joint specimen conditioned for 42 days at 70^{o}C/85% relative humidity and tested in static tension. (x24 magnification).

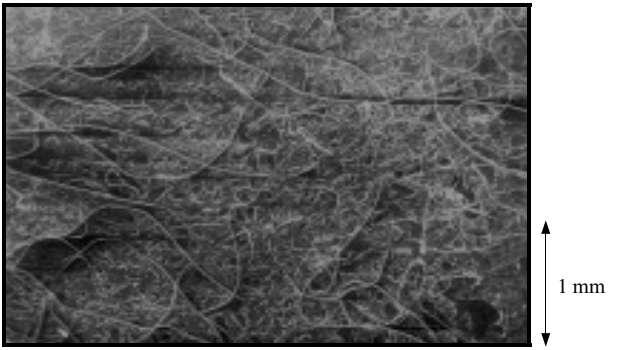

Figure 34 Typical fracture surface of an Al 5251/AF126 tapered-strap joint specimen conditioned for 42 days at 70^{o}C/85% relative humidity and tested at 55% tensile fatigue followed by static tension (x24 magnification).

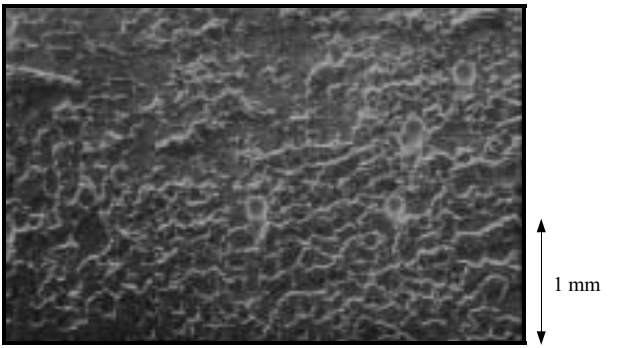

Figure 35 Typical fracture surface of an Al 5251/AV119 TAST specimen tested in static tension - no conditioning. (x24 magnification).

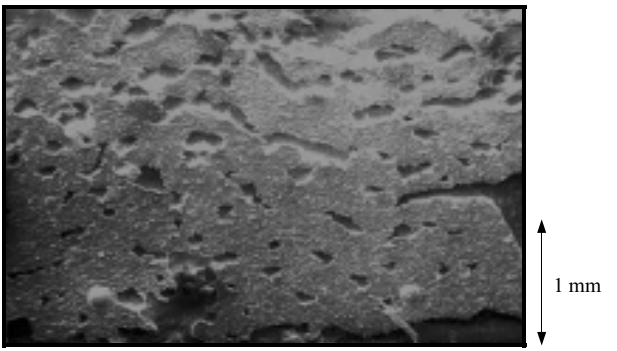

Figure 36 Typical fracture surface of an Al 5251/AV119 TAST specimen tested in static tension - no conditioning. (x24 magnification).

Figure 37 Typical fracture surface of an Al 5251/AV119 TAST specimen tested in static tension - no conditioning. (x24 magnification).

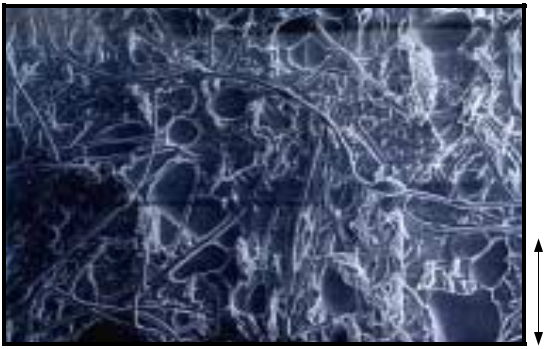

Figure 38 Typical fracture surface of an Al 5251/AF126 TAST specimen tested in static tension - no conditioning. (x75 magnification).

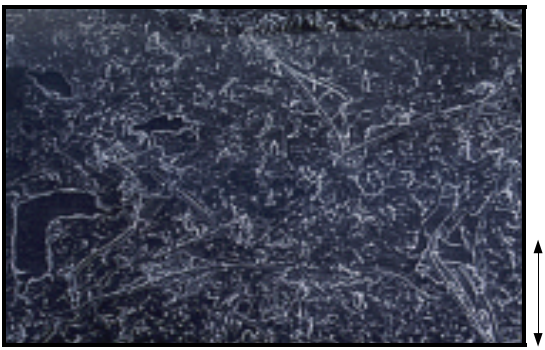

Figure 39 Typical fracture surface of an Al 5251/AF126 TAST specimen tested in static tension after 42 days water immersion at 25^{o} C. (x75 magnification).

Figure 40 Typical fracture surface of an Al 5251/AF126 TAST specimen tested in static tension after 42 days water immersion at 60^{o} C. (x75 magnification).

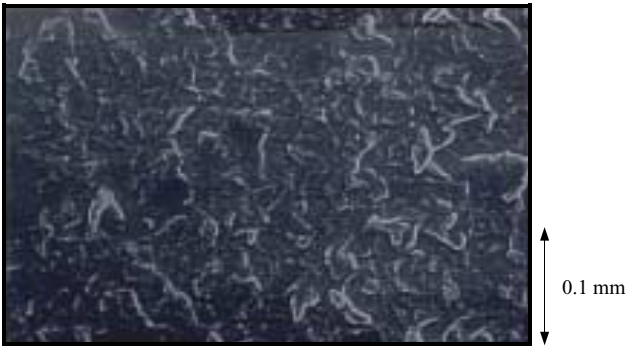

Figure 41 Typical fracture surface of an Al 5251/F241 TAST specimen tested in static tension - no conditioning. (x250 magnification).

Figure 42 Typical fracture surface of an Al 5251/F241 TAST specimen tested in static tension after 42 days water immersion at 25^{o}C. (x250 magnification).

Figure 43 Typical fracture surface of an Al 5251/F241 TAST specimen tested in static tension after 42 days water immersion at 60^{o}C. (x250 magnification).

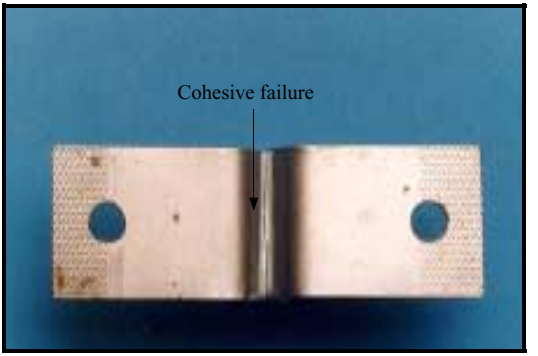

Figure 44 Cohesive failure in the adhesive fillet of a CR1 mild steel/AV119 T-peel joint.

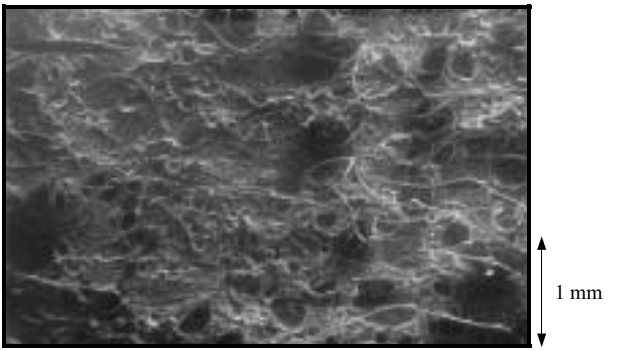

Figure 45 Typical fracture surface of an Al 5251/AF126-2 scarf joint tested in static tension. (x24 magnification)

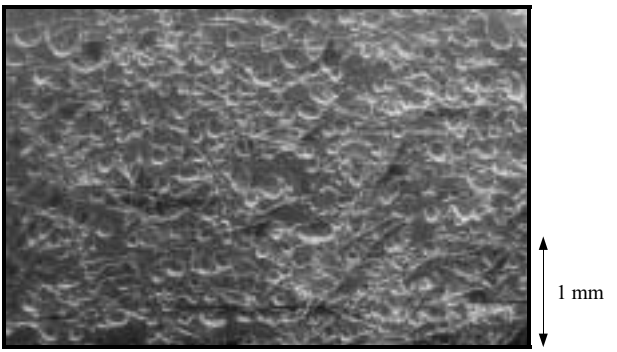

Figure 46 Typical fracture surface of an Al 5251/AF126-2 scarf joint tested in 85% UTS tensile fatigue. (x24 magnification)

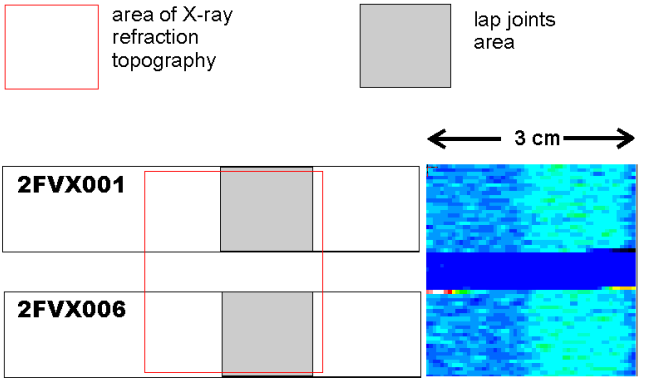

(a) transverse inspection, 2FVX001 conditioned (upper sample)/2FVX006 unconditioned;
(beam vertical to drawing plane)

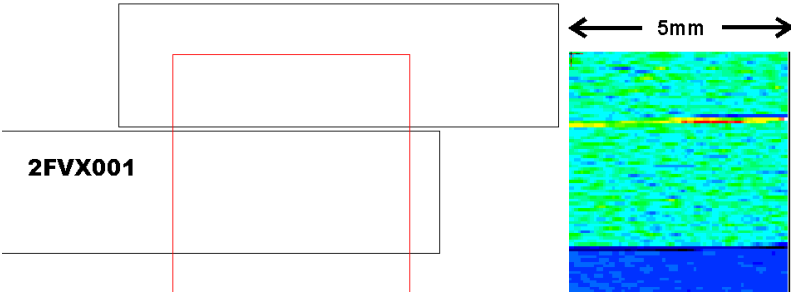

(b) conditioned specimen, beam parallel to joint plane (vertical to drawing plane)

Figure 47 Exploratory X-ray refraction results for CFRP composite single lap joints.